PROCEEDINGS of the
23rd International Congress on Acoustics
9 to 13 September 2019 in Aachen, Germany

Design and simulation of a benchmark room for room acoustic auralizations

Fotis Georgiou[(1)], Baltazar Briere de la Hosseraye[(1)], Maarten Hornikx[(1)], Philip Robinson[(2)]

[(1)]Eindhoven University of Technology, The Netherlands, f.georgiou@tue.nl
[(2)]Facebook&Oculus, U.S.A., philrob22@fb.com

Abstract
In order to achieve accurate acoustic simulations of a room for obtaining an authentic auralization, the following aspects need to be quantified: the geometrical details of the room, all material properties and the characteristics of the source and the receiver. This paper presents the design of a benchmark room for this purpose, including all this information. The room is a building acoustics transmission chamber with thick concrete walls. This room was then acoustically treated to achieve an acoustic environment close to a day-to-day office room. The surface impedances of the materials additionally installed in the room were measured with both in the impedance tube as well as with a pressure-velocity sensor. Furthermore, the directivity of the measurement source and the binaural receiver were measured in order to be included in the simulations. Impulse responses of this benchmark room have also been obtained from simulations with the in-house time-domain discontinuous Galerkin method (DG) with frequency-dependent boundary conditions, including source and receiver directivity. Time and frequency domain results from the both the measurements and simulations are presented, showing a close agreement.

Keywords: Auralization, Room acoustics, Acoustic modeling, Discontinuous-Galerkin

1 INTRODUCTION

Auralization can be a valuable tool for architectural acoustics as it provides more information regarding the acoustics of an indoor space compared to standardized room acoustic parameters such as RT60, C80 and STI (1, 2). With auralization, all the sound sources present in the environment can be simulated, and it can be used to characterize the space with psychoacoustic metrics. Also, auralization can be a great communication tool (2).

Even though the concepts of auralization and acoustic modeling have been introduced over 6 decades ago (3), there are still many open questions. One of the key unanswered questions is how close the results of a computer simulation can get to a real-life acoustic environment. This question does not only relate to the acoustic modeling method itself but also to the input parameters in the model, such as the acoustic properties of the materials within the modeled space and the characteristics of source and receiver.

Room acoustic modeling has been achieved with various methods. These methods can be split into three categories: geometrical acoustics methods, energy-based methods, and wave-based methods.

Wave-based methods are techniques used to solve the governing partial differential equation(s) with numerical approximations. Wave-based methods are physically accurate and inherently include complex wave-phenomena such as diffraction (also modeled with high accuracy) (4). This is the main advantage of the wave-based methods compared to the geometrical acoustics methods. Among the wave-based methods are FDTD (5), the boundary element method (BEM) (6), the finite element method (FEM) (7), the digital waveguide mesh (DWM) (8), the finite-volume method (9) and the discontinuous Galerkin (DG) method (10). The main disadvantage of these methods is that they are computationally expensive. When the high frequency limit of the simulation is increased, the discretization step in space (and time) needs to be decreased, which results in an increase of the computational load. Therefore, they become impractical at high frequencies (11).

In order evaluate the quality of a room acoustic simulation model all the geometrical details of the room, furniture, material properties as well as the source and receiver characteristics need to be known in order to incorporate them inside the modeling method and compare the results against the measurements of that room. This is very difficult to do in an existing room because of the following reasons: 1) it is difficult to quantify the acoustics properties of the materials in-situ, 2) the room might include materials that are very difficult to include in the acoustic simulations. Therefore, the design a of benchmark room, with a relatively simple yet realistic

geometry that will be treated with acoustic materials that can be accurately quantified, is of high importance.

There are a number of papers that focused on the design and measurement of a reference/benchmark room together with material measurements in order to evaluate different modeling approaches by comparing them to the reference measurements such as (12, 13) and some of them also in the context of auralization (14). Moreover, some interesting review papers on this subject have appeared (1, 4, 15). The main outcomes are: 1) the input material data is very important, 2) the geometrical methods fail to produce IRs equivalent to the measured ones especially at low frequencies because they cannot model diffraction and modal interferences, 3) the low frequencies can be modeled accurately using a wave-based method but due the fact that they become computationally expensive at high frequencies they can only be used for a limited frequency range. Hybrid approaches that use wave-based method for low frequencies and geometrical acoustics method for high frequencies have been developed but there is no standardized methodology yet on how to do this (11). Also, there are still open questions such as where the cross-fade frequency between the wave-based and the geometrical acoustics method should be.

The main objective of the research presented in this paper is to obtain measurements from a benchmark room for auralization purposes and compare them with results from a high-frequency wave-based simulation method. In the work presented in this paper the wave-based method is applied to a higher frequency range (2.5 kHz) than in previous works. Moreover, in this research a benchmark room was designed and all the material properties were measured both in the impedance tube and with the pressure-velocity (PU) sensor. In previous works (12–14) reserachers made use of real-rooms, thus, they could not extract the acoustics properties from all the room's materials.

The reason that a wave-based method was used for the acoustic modeling is because such an accurate method may answer how close the results of a computer simulation can get to a real-life acoustic environment. Therefore, it was decided to run a DG simulation up to approximately 2.5 kHz and compare the results against the measured IRs. DG is used because it is able to handle complex geometries by discretizing the room volume by non-overlapping mesh elements, and it allows to model time-domain frequency dependent boundary conditions (16).

This paper starts by presenting the design of the benchmark room. Next, the impulse responses (IR) and the binaural room impulse responses (BRIRs) measurements inside that room are demonstrated. Finally, the results from the DG simulations are presented against the measurements.

2 DESIGN OF THE BENCHMARK ROOM

The empty building acoustics transmission chamber in the Echo building at Eindhoven University of Technology, which has a geometry that can easily be meshed for a solution by the DG method, was chosen to be modified as the benchmark room. The reverberation time of the empty building acoustics transmission chamber is very high, ranging from 7.6 s down to 2.7 s between 125 Hz - 4000 Hz. At even lower frequencies, the reverberation time is exceeding the 10 s. The reverberation time is rather homogeneous for different source-receiver (S-R) configurations withing the room from the 1000 Hz band and up, but is not at lower octave-bands due to the influence of the room modes at low frequencies.

This empty room was acoustically treated to achieve two room acoustic scenarios. The goal of Scenario 1 was to achieve the acoustics of a typical office room, with a reverberation time in the range of 0.5 s to 0.8 s over the 125 - 4000 Hz octave-bands. Scenario 2 was designed as an office room with "bad acoustics". While the reverberation time of Scenario 2 should not be as extreme as the one of the empty reference room, it was designed to be significantly longer (in the range of 1.0 s to 1.3 s over the 125 - 4000 Hz octave-bands) to reduce the speech intelligibility within the room.

The furniture and the materials that were placed inside the empty room had geometries that could be easily incorporated in the DG mesh. Two type of absorbing materials were chosen for the acoustic treatment of the room: porous materials for the wall panels and carpet tiles to cover the ground surface (see (17) for more information regarding the material properties). These materials were chosen because they act as locally reacting surfaces, which is important for their accurate modeling in the numerical simulations in DG. The furniture was

placed to create some scattering in order to break down some room modes.

The geometry of Scenario 1 is shown in Figure 1. The uncertainty of the measured distances is estimated to be smaller than 5 cm. The orientation of the objects (chairs, tables, lockers) was also marked on the floor using gaffer tape. Finally, the locations and geometries of the objects were reconstructed in SketchUp models. The origin of the coordinate system in the SketchUp models is the left bottom corner (see Figure 1). Scenario 2 was set-up by removing several elements which were present in the room for Scenario 1. The floor was left with 11 m^2 carpet tiles and the walls were left with 6 absorbing panels. The furniture in the room was also reduced to 3 chairs and 2 tables. The ceiling remained untreated in both scenarios.

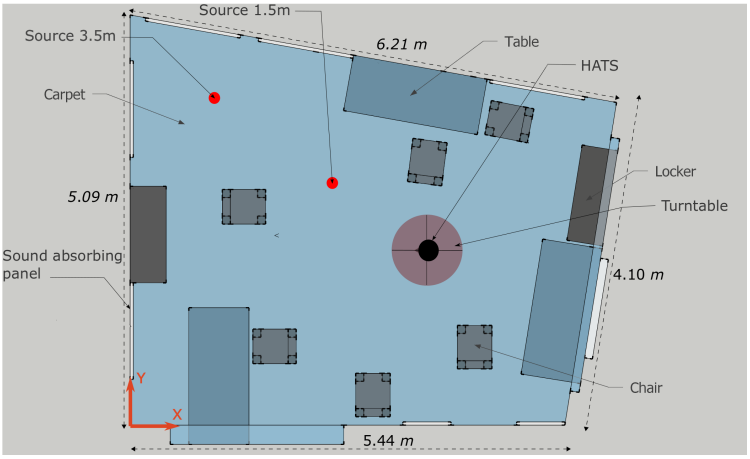

Figure 1. Top view of Scenario 1 including the source and receiver positions.

3 IR, BRIR, SOURCE DIRECTIVITY, HRTF, AND MATERIAL PROPERTIES MEASUREMENTS

For each of the two room acoustic scenarios, measurements were performed with two different sound sources using the B&K TYPE 4295 omnisource. The HATS was mounted on the turntable and its location was kept the same at all measurements. The BRIRs were captured with a full rotation (360°) in the horizontal plane with 5° angular resolution, and for 2 different source-receiver configurations with distances of 1.50 m and 3.50 m (see Figure 1). The omnisource's top opening was positioned at ear height facing the ceiling.

The measurements were carried out during evening and night time, in order to avoid noise disturbances from the nearby offices. The temperature in the room during the measurements was very stable ($T = 21.6 \pm 0.3$ $^{\circ}C$), and varied slightly from one day to another. The following measurement equipment was used: B&K 4128-C HATS, B&K 1/2-inch free-field microphone 4189, Dell latitude E5530 laptop with Windows 10, Acoustics Engineering-Amphion power amplifier and Acoustics Engineering-Triton +10 dB gain sound card. The measurement were conducted using the Acoustics Engineering-Dirac 6 acoustics measurement software. An exponential sine-sweep of 175 s long was used as a measurement signal to achieve high signal-to-noise ratio.

The impulse-to-noise ratios (INRs)[1] obtained from the measured BRIRs were within the range of 75 - 93 dB for the octave-bands 63 - 8000 Hz (see Figures 2), implying a very high quality of the measurements. An initial analysis showed that the reverberation times at low frequencies (below 125 Hz) were very high. It was not possible to reduce the low-frequency reverberation times below 1 - 1.5 s (see Table 1), which was one of the design goals. Attempts for further room treatment were made, which achieved a significant reverberation time reduction at low frequencies. However, these treatments included objects that would be very difficult to model in the numerical simulations, as they act as non-locally reacting surfaces. Thus, it was decided not to

[1]INR is equal to the maximum root-mean-square (RMS) level of the room impulse response (in dB) minus the noise level (in dB) (18).

not add any extra objects in room other than the ones shown in Figure 1.

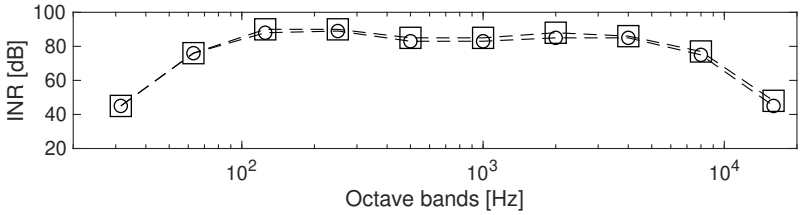

Figure 2. INR of right ear BRIRs Scenario 1 measured at 0° for S-R distance 1.5 m (triangles) and 3.5 m (circles).

The HRTFs of the B&K 4128-C HATS and the directivity of the B&K TYPE 4295 omnisource where measured inside a semi-ancechoic chamber. The surface impedances of the carpet tiles and the sound absorbing panels where measured both with the impedance tube and the pressure-velocity (PU) probe. More details regarding the impedance measurements can be found in (17).

4 DG SIMULATIONS AND COMPARISON AGAINST THE MEASUREMENTS

4.1 DG simulations

The measured IRs and BRIRs were computed with the in-house DG MATLAB code, which is described in detail in (10). Because of the large unevenness of the reverberation times between the low and high octave-bands (see Figure 1), it was decided to run two sets of computations, a 12 s long calculation for the low frequency range ("LF", up to 500 Hz) and a shorter one of 0.6 s long for the more computationally expensive mid-to-high frequency range ("HF", from 500 Hz to 2.5 kHz) respectively and then combine them (see Subsection 4.4).

The meshes of the various scenarios were created from the Sketchup models of the geometry via the software Gmsh. For the two sets of simulations, the characteristic length L_c, was set to the half of the wavelength corresponding to the maximum simulated frequency f_{max} ($L_c = c/(2f_{max})$, where c is the speed of sound). For the LF simulations f_{max} was set at 500 Hz and for the HF at 2500 Hz. In order to ensure accurate results up to these frequencies, a polynomial order $N = 4$ was used in the DG simulations to obtain more than 10 degrees of freedom per wavelength. Unfortunately, the post-analysis showed that the size of the elements of the DG mesh for the HF simulations was not small enough to simulate the initial Gaussian distribution properly, which gave directional characteristics in the initial condition. Therefore, the pressure from the initial condition was not distributed equally in each direction causing directivity fluctuations $<$6 dB.

4.2 Boundary conditions

The frequency dependent time-domain boundary conditions (TDBCs) used in the simulation are the ones derived in (17) for the carpet and the porous panel. They were applied to the relevant surfaces via the physical surfaces definition tool in the Gmsh software. The hard walls of the room were assumed to behave as frequency-independent reflective surfaces with a real reflection coefficient. This acoustic reflection factor was set to $R = 0.991$, in accordance with a previous measurement of the empty room described in Section IV.D in (10), where this reflection coefficient was derived from the quality factor of the strong modal resonance at 97.9 Hz.

4.3 Source and receivers

The source directivity of the measurement source was not incorporated in the simulations due to an issue with the measured directivity data and was left for future work. The simulated source was an omnidirectional Gaussian pulse, with a different source width for low and high frequency simulations. In order to reproduce the auralization binaurally via headphones allowing for head rotations, binaural responses need to be rendered from the DG simulations. This was implemented by storing the sound field over a dual spherical array of receiver

locations, placed in the simulation domain. The receiver points consisted of two concentric spheres, an inner sphere and and outer sphere, following the approach presented in (19). Next, spherical harmonics were applied together with the database of measured HRIRs from the HATS used in the measurements, to post-process the data to HRIRs for the same set of head rotations as used in the measurements.

4.4 IRs and BRIRs post-processing and combination of low and high frequency IRs and BRIRs

The calculations of the modeled IRs and BRIRs include the spectral characteristics of the initial condition, which is a Gaussian distribution. A correction (equalization) filter was designed to correct for the Gaussian spectrum based on the method presented in (20). Since two separate simulations were conducted, one for the low and one for the high frequencies, two inverse filters had to be designed using the free-field time responses of the low and high frequency Gaussian initial conditions.

The method developed in Section 4.3 in (11) was used to combine the low and high frequency IRs and BRIRs. The only difference with (11) is that the combination was made in the time-domain and not in the frequency-domain. The method is demonstrated in Figure 3. First, the cross-fade frequency between the low and the high frequency simulations needs to be decided based on the limit of the low-frequency simulations. In all the simulations presented in this report the cross-fade frequency was 500 Hz because the reverberation tails from this octave-band and above were included in the high frequency simulations, which were much shorter in duration compared to the low-frequency ones (see Section 4.1). Next, the low and the high frequency simulations were filtered with a 9^{th} order zero-phase low-pass and high-pass filter respectively and the outputs are summed together. The filters were designed using the *butteworth.m* function in Matlab and the zero-phase filtering was performed using the *filtfilt.m* function. The reason for performing zero-phase filtering and not normal filtering is that the normal Butterworth filters cause a frequency-dependent delay and in order to avoid this zero-phase filtering was applied. However, (11) states that the frequency-dependent delay does not add any audible artefacts in the IRs. Finally, a 8^{th} order (normal) Butterworth low-pass filter was applied to the combined output with a cut-off frequency that depends on the accuracy limit of the high-frequency simulations, which for the simulations presented here is estimated to be around 2.1 kHz.

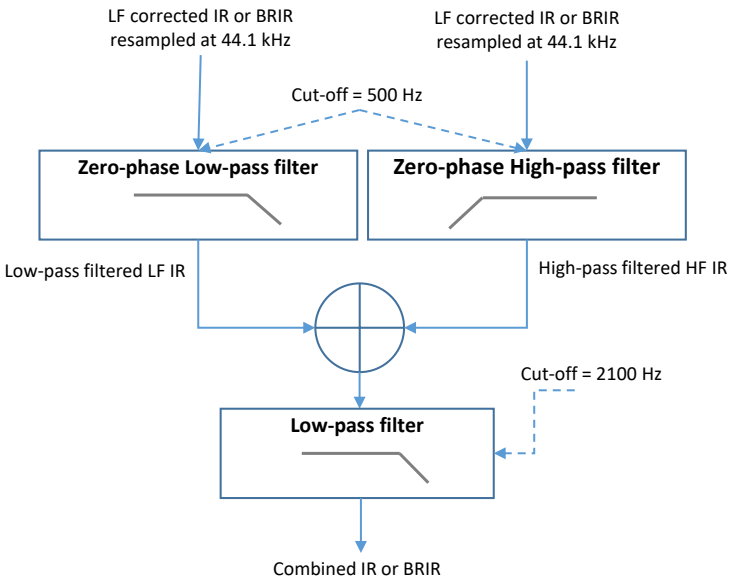

Figure 3. Flow chart of the combination of the low frequency (LF) and high frequency (HF) IRs.

4.5 Measurement versus Simulations

In Figure 4 the measured IR of Scenario 1 for S-R distance 1.50 m is plotted against the simulated IR. The matching at low frequencies is very good except from a big deep in the frequency response present in the measured IR at approximately 53 Hz. At high frequencies the errors are larger because: 1) the issue with the large element size in the high frequency simulations, which is discussed in Section 4.1, 2) the directivity of the B&K TYPE 4295 omnisource, which is not a perfect omnidirectional source above the 1 kHz octave-band, was not included in the simulations. Regarding the IRs (time response), the matching is good but they are not identical. The biggest difference is in the direct sound component.

In Table 1, the measured and simulated T20s of Scenario 1 and 2 are plotted. In Scenario 1 the matching is very good at 500 Hz and at 1000 Hz octave-bands and in Scenario 2 the matching is very good between 250 - 1000 Hz octave-bands. At low frequencies the mismatch is very large in both scenarios. This mismatch is possibly caused by an inaccuracy of the TDBCs at low frequencies, especially below 100 Hz, where reliable measurements of the materials' properties could not be performed. The reflective nature of the materials in this frequency range is potentially aggravating further the relative error in the measured absorption coefficients.

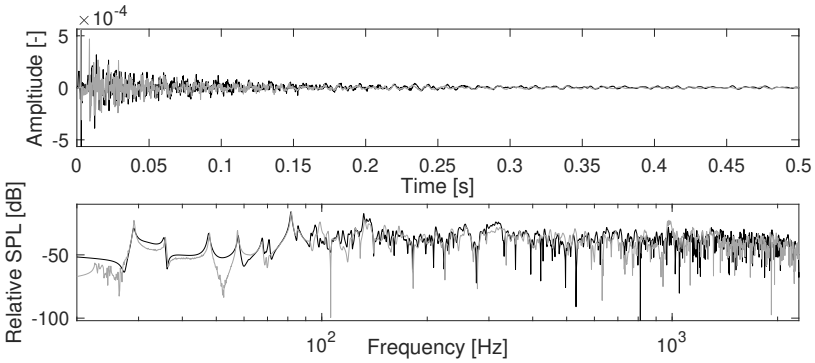

Figure 4. Time (top) and frequency (bottom) response of the measured (grey) vs the simulated (black) IR of room Scenario 1 for S-R distance 1.50 m. Only the 0.5 s of the time responses are shown here, however, the frequency responses are computed using the full 12 s of time signals.

Table 1. Measured vs simulated T20s in Scenario 1 (S1) and Scenario 2 (S2).

Octave-bands (Hz)	**63**	**125**	**250**	**500**	**1000**	**2000**
Measured T20 in S1 (s)	5.98	1.58	0.67	0.47	0.47	0.49
Simulated T20 in S1 (s)	3.45	2.11	0.98	0.55	0.51	0.38
Measured T20 in S2 (s)	8.80	3.71	1.68	0.86	0.76	0.87
Simulated T20 in S2 (s)	4.02	2.84	1.64	0.93	0.73	0.56

In Figure 5 the right ear simulated BRIR of room Scenario 2 at 0° for S-R distance 3.50 m is plotted against the measurement. The results show a similar degree of accuracy at high frequencies as the IR presented in Figure 4. However, there is a bigger error at low frequencies because the HRTFs used in the spherical harmonic approach to obtain the computed BRIRs are plane wave functions (see Subsection 4.3) and for nearby sources this introduces some low frequency errors.

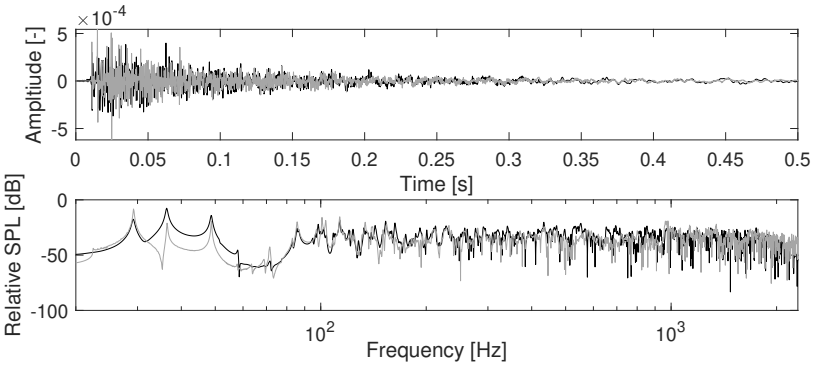

Figure 5. Time (top) and frequency (bottom) response of the measured (grey) vs the simulated (black) right ear BRIR of room scenario 2 for S-R distance 3.50 m and at 0°. Only the 0.5 s of the time responses are shown here, however, the frequency responses are computed using the full 12 s of time signals.

5 CONCLUSIONS AND FUTURE WORK

This paper presented the measurements in a benchmark room designed for auralization purposes, and includes results from the room acoustics simulations using the wave-based DG method. All details from the the measurement room were captured as input data for simulation methods. The results showed a good match between the measurements and the simulations. However, refinement of both the input (proper source directivity data) as simulations (improving the modelled source function in DG, using source directivity, using higher order spherical harmonics for post-processing the BRIRs) is foreseen to further improve the benchmark room dataset as well as the wave-based results. Moreover, apart from the objective comparisons, subjective evaluations also need to be conducted in order to investigate how much the measurements and the simulations differ from the perceptual point of view.

ACKNOWLEDGEMENTS

This work was supported in part by funding from Facebook Technologies, LLC.

REFERENCES

1. Vorländer, M.; et al. Virtual reality for architectural acoustics, Journal of Building Performance Simulation, Vol 8, 2014, pp. 15–25.
2. Azevedo, M.; Sacks, J. Auralization as an architectural design tool. Proceedings of the EAA Joint Symposium on Auralization and Ambisonics, Berlin, Germany, April 2014.
3. Schröder, M.; Atal, B. S.; Bird, C. Digital computers in room acoustics. Proceedings of the 4th International Congress on Acoustics, Copenhagen, Denmark 1962, pp. M21.
4. Välimäki, V.; et al. Fifty years of artificial reverberation, IEEE Transactions on Audio, Speech and Language Processing, Vol 20, 2012, 1421–48.
5. Kowalczyk, K.; Van Walstijn, M. Room acoustics simulation using 3-D compact explicit FDTD schemes,IEEE Transactions on Audio, Speech and Language Processing, Vol 19, 2011, pp. 34–46.
6. Kirkup S. The boundary element method in acoustics. Integrated Sound Software, 2007.
7. Thompson, L. L. A review of finite element methods for time-harmonic acoustics. The Journal of the Acoustical Society of America 119, Vol 3, 2006, pp. 1315–1330.
8. Murphy, D. T. Digital waveguide mesh topologies in room acoustics modelling. PhD thesis, The University of York, 2000.
9. Bilbao, S.; Hamilton, B.; Botts, J; Savioja, L., 2016. Finite volume time domain room acoustics simulation

under general impedance boundary conditions. IEEE/ACM Transactions on Audio, Speech, and Language Processing, Vol 24(1), pp.161-173.
10. Wang, H.; Sihar, I.; Pagán Muñoz, R.; Hornikx, M. Room acoustics modelling in the time-domain with the nodal discontinuous Galerkin method, The Journal of the Acoustical Society of America, Vol 145(4), 2019, pp. 2650–2663.
11. Aretz, M. Combine wave and ray based room acoustic simulations of small rooms. PhD thesis, RWTH Aachen University, 2012.
12. Bork, I. A Comparison of Room Simulation Software - The 2nd Round Robin, Acta Acustica United with Acustica, Vol 86, 2000, pp. 943–956.
13. Bork, I. Report on the 3rd Round Robin on Room Acoustical Computer Simulation - Part II: Calculations, Acta Acustica United with Acustica, Vol 9, 2005, pp. 753–763.
14. Brinkmann, F.; et al. A round robin on room acoustical simulation and auralization, The Journal of the Acoustical Society of America, Vol 145 (4), 2019, pp. 2746-2760.
15. Vorländer, M. Computer simulations in room acoustics: concepts and uncertainties, The Journal of the Acoustical Society of America, Vol 133, 2013, pp. 1203–13.
16. Wang, H.; Hornikx, M. Broadband time-domain impedance boundary modeling with the discontinuous Galerkin method for room acoustics simulations, Proceedings of International Congress on Acoustics, Aachen, Germany, September 2019.
17. Briere de La Hosseraye, B.; et al. Implementation of frequency dependent time-domain boundary conditions based on in-situ surface measurements and model fitting, Proceedings of International Congress on Acoustics, Aachen, Germany, September 2019.
18. Acoustics Engineering, Impulse to noise ratio: Qualification Parameter For Acoustical Impulse Response Measurement, Technical report, 2002.
19. Rafaely, B. Springer Topics in Signal Processing Fundamentals of Spherical Array Processing, 2015.
20. Gardner, W.G. 3-D audio using loudspeakers. Springer US, 1998.